Chapter 47
High Sensitivity Mach–Zehnder Interferometer for Sub-Nanoliter Liquid Sensing

G. Testa, L. Zeni, Yujian Huang, P. M. Sarro and R. Bernini

Abstract In this paper we present a new configuration of an integrated optofluidic Mach–Zehnder interferometer based on liquid core ARROW waveguide that permits to obtain high sensitivity for liquid sensing. The proposed devices have been realized and optically characterized. The experimental results are in good agreement with the theoretical ones.

47.1 Introduction

Integrated Mach–Zehnder (MZ) interferometers are very powerful optical sensor device, able to detect low refractive index changes with very high accuracy.

Due to the well-known sensing capabilities, these devices are widely applied in chemical and biochemical applications, where the sensing is performed on sample dispersed in liquid. In the last few years new configurations, capable to enhance the optical sensitivity of these devices, have been proposed [1, 2]. One possible approach to improve the sensitivity is to employ liquid core waveguides. In comparison to conventional MZI, liquid core MZI offers the advantage to have an improved sensitivity due to the direct optical coupling of the light with the liquid sample. Such a new optofluidic configuration has recently attracted much attention and some examples of liquid interferometers have been reported [2, 3].

G. Testa · R. Bernini (✉)
IREA-CNR, Via Diocleziano 320, 80124 Naples, Italy
e-mail: bernini.r@irea.cnr.it

L. Zeni
DII Seconda Università di Napoli, Via Roma 29, 81031 Aversa, Italy

Y. Huang · P. M. Sarro
ECTM-DIMES, TUDelft. NL, 2600, GB, Delft, The Netherlands

G. Neri et al. (eds.), *Sensors and Microsystems*,
Lecture Notes in Electrical Engineering 91, DOI: 10.1007/978-94-007-1324-6_47,

The use of liquid core waveguide permits to maximize the partial sensitivity of the interferometer, defined as the rate of change of the effective refractive index of the guided mode as the liquids index varies. In this case, since the mode field is almost completely confined into the liquid core of the waveguide, the coupling between sample and light is very strong, leading to a partial sensitivity that can approach to one. Recently our group have proposed an optofluidic Mach–Zehnder interferometer based on liquid core ARROW waveguide [3]. However, the asymmetric geometry induces a low visibility of the interferometer with a strong degradation of the device's performances, which became even more evident by increasing the sensing length.

Here we demonstrate that with an accurate design of the device geometry, it is possible a great improvement of interferometer's visibility also for highly asymmetric Mach–Zehnder configurations, improving in this way the overall sensitivity of the device [4].

47.2 Operating Principle

The proposed interferometer has been realized with liquid ARROW waveguides. ARROW waveguides are able to confine the light into the liquid core by high reflectivity Fabry–Perot mirror composing the waveguide claddings. By choosing the appropriate cladding materials, we have designed the waveguide to perform low loss propagation at $\lambda = 635$ nm with a core refractive index of $n_c = 1.33$.

The fabricated ARROW has been realized in silicon [5]. The waveguide channels shaping the interferometer have been etched on the bottom silicon wafer by mask lithography. The high index contrast cladding layers thicknesses have been chosen in order to minimize the propagation loss [5]. The first cladding is composed by a titanium dioxide layer $(n_1 = 2.49)$ with a thickness of $d_1 = 75.4$ nm deposited by atomic layer deposition. The second cladding is silicon dioxide layer $(n_2 = 1.46)$ and it has been deposited by LPCVD $(d_2 = 262\,\text{nm})$. The liquid into the core was infiltrated by capillary effect (methanol, $n_c = 1.32$).

The visibility of a MZI is strictly related to the polarization and the intensity balancing between the beams emerging from the two arms of the interferometer. The filtering properties of the ARROW in terms of polarization permit to get the interfering beams with the same polarization (TE) independently to input polarization [3]. Hence, to achieve a good visibility factor we modified the shape of the arms in order to balance, as well as possible, the intensity of the interfering beams. A schematic layout of the proposed device is showed in Fig. 47.1.

The device is composed by an input straight waveguide, followed by a taper waveguide ending into a T-branch that splits equally the input power into the two arms of the interferometer. The final width of the taper has been set to 20 μm in order to get the fundamental guided mode substantially widened for matching the width of the input port of the T-branch. Moreover, by numerical simulations, we have found that a length of the taper of 500 μm permits us to realize a slowly

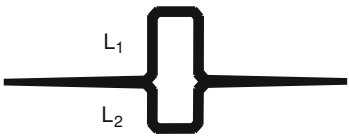

Fig. 47.1 Schematic layout of the MZI

varying tapered waveguide so as to avoid the propagation of higher-order modes and to maximize the power coupling of the fundamental input mode with the fundamental mode of the output waveguide. Each 90°-bent waveguides composing the two arms of the MZI consists of cut-type bends. After propagating in the two arms (L_1, L_2), the emerging beams accumulate a phase difference given by

$$\Delta\varphi = \frac{2\pi}{\lambda} n_{eff}(L_1 - L_2) \tag{47.1}$$

where n_{eff} is the effective index of the fundamental propagating mode and λ is the working wavelength. Since liquid waveguides compose the device, a length difference $\Delta L = L_1 - L_2$ between the two arms is required to achieve a phase delay between beams at the output. The transmitted intensity from the device is given by

$$I \propto 1 + V\cos(\Delta\varphi), \tag{47.2}$$

where the phase difference $\Delta\varphi$ is given by Eq. 47.1, $V = (\mathrm{I_{max}} - \mathrm{I_{min}})/(\mathrm{I_{max}} + \mathrm{I_{min}})$ is the visibility of the interferometer. In the proposed layout, the intensity unbalance between interfering beams is only due to the different length of the straight waveguides of the arms that causes different propagation loss.

47.3 Experimental Results

We have fabricated and optically characterized two unbalanced MZ configurations ($\mathrm{MZ_1}$ and $\mathrm{MZ_2}$) with different sensing length ΔL by varying the separation between arms. In the $\mathrm{MZ_1}$ configuration the sensing length is $\Delta L_1 = 100\,\mu\mathrm{m}$, while for $\mathrm{MZ_2}$ it is $\Delta L_2 = 200\,\mu\mathrm{m}$. The total length of the devices is 2.5 mm and the required volume is about160 pl.

In Fig. 47.2 is shown a scanning electron microscope image of the MZI.

The free-spectral range (FSR) of the interferometer, defined as the spectral distance between two adjacent maxima (minima) in the interference pattern, have been theoretically estimated, resulting in $\mathrm{FSR_1} = 3$ nm and $\mathrm{FSR_2} = 1.52$ nm for $\mathrm{MZ_1}$ and $\mathrm{MZ_2}$, respectively. In Fig. 47.3 the normalized transmitted spectrum from $\mathrm{MZ_1}$ (a) and $\mathrm{MZ_2}$ (b) are shown. From the measured spectra we have evaluated a FSR at around $\lambda = 640$ nm of $\mathrm{FSR_1} = 2.80$ nm and of $\mathrm{FSR_2} = 1.48$ nm; in good agreement with the theoretical ones.

The visibility of the fringes measured from the transmitted interferometric pattern is $V_1 = 0.990$ for $\mathrm{MZ_1}$ and $V_2 = 0.977$ for $\mathrm{MZ_2}$. By taken into account the attenuation losses of the fabricated liquid ARROWs [5], a visibility of about

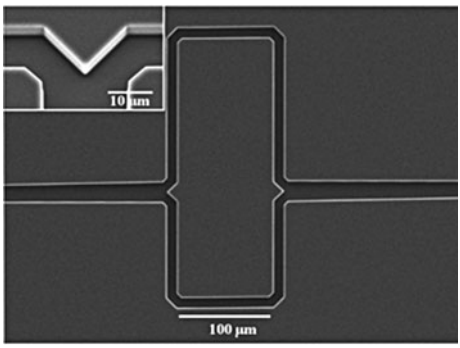

Fig. 47.2 SEM picture of the fabricated device. Inset, detail of the T-branch

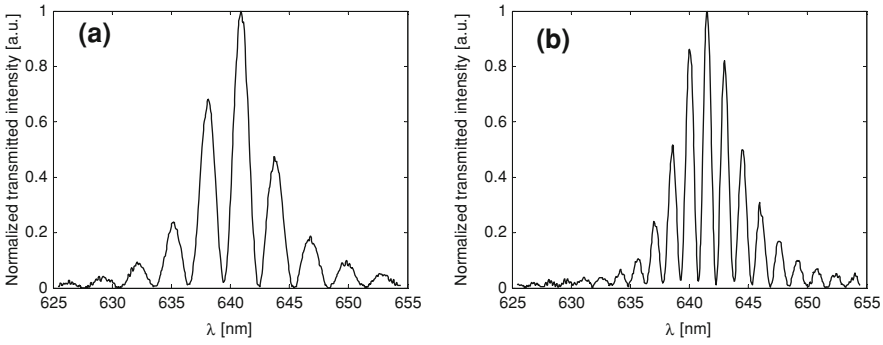

Fig. 47.3 Measured transmitted spectra from MZ_1 (**a**) and MZ_2 (**b**), FSR1 $\Delta\lambda \sim 3$ nm, FSR_2 $\Delta\lambda \sim 1.52$ nm

99.9% is theoretically calculated for both MZ_1 and MZ_2. These values agree well with the measured ones. This MZ interferometer can be applied as high sensitivity optical sensor. If the liquid core refractive index changes, a variation of the optical output power can be detected at fixed wavelength; the estimated sensitivity is 10^{-6} RIU, around $\lambda = 640$ nm and at $n_c = 1.33$ for MZ_2.

Acknowledgments The authors thank the IC Process Group of DIMES for help in device fabrication.

References

1. Densmore A, Xu DX, Janz S, Waldron P, Mischki T, Lopinski G, Delâge A, Lapointe J, Cheben P, Lamontagne B, Schmid JH (2008) Spiral-path high-sensitivity silicon photonic wire molecular sensor with temperature-independent response. Opt Lett 33:596–598
2. Dumais P, Callender CL, Noad JP, Ledderhof CJ (2008) Integrated optical sensor using a liquid-core waveguide in a Mach–Zehnder interferometer. Opt Express 16:18164–18172
3. Bernini R, Testa G, Zeni L, Sarro PM (2008) Integrated optofluidic Mach–Zehnder interferometer based on liquid core waveguides. Appl Phys Lett 93:011106–011109

4. Testa G, Huang Y, Zeni L, Sarro PM, Bernini R (2010) High-visibility optofluidic Mach–Zehnder interferometer. Opt Lett 35:1584–1586
5. Testa G, Huang Y, Zeni L, Sarro PM, Bernini R (2010) Liquid core ARROW waveguides by atomic layer deposition. IEEE Photon Technol Lett 22:616–618